Ab initio theoretical description of the dependence of magnetocrystalline anisotropy on both compositional order and lattice distortion in transition metal alloys

S. S. A. Razee and J. B. Staunton
Department of Physics, University of Warwick, Coventry CV4 7AL, United Kingdom

B. Ginatempo and E. Bruno
Dipartimento di Fisica and Unità INFM, Università di Messina, Salita Sperone 31, I-98166 Messina, Italy

F. J. Pinski
Department of Physics, University of Cincinnati, Cincinnati, Ohio 45221

(Received 21 August 2000; published 11 June 2001)

Recently, we outlined a scheme to investigate the effects of both short-ranged and long-ranged compositional order on the magnetocrystalline anisotropy of alloys from a first-principles electronic structure point of view [Phys. Rev. Lett. **82**, 5369 (1999)] and showed that in the $Co_{0.5}Pt_{0.5}$ alloy compositional order enhances the magnitude of magnetocrystalline anisotropy energy (MAE) by some two orders of magnitude. Here we describe our scheme in detail and study some more transition metal alloys. In the $Co_{0.25}Pt_{0.75}$ alloy we find the perfect $L1_2$ structure to be magnetically soft whereas imposition of directional order greatly enhances its MAE. We also present the effect of lattice distortion (tetragonalization) on MAE on the same footing and find that in the $Co_{0.5}Pt_{0.5}$ alloy it accounts for only about 20% of the observed enhancement, thus confirming that compositional order is the major player in this effect. Tetragonalization of the lattice has also a modest effect on the MAE of the $Fe_{0.5}Co_{0.5}$ alloy. We also examine the electronic effects which underpin the directional chemical order that is produced by magnetic annealing of permalloy which we study within the same framework.

DOI: 10.1103/PhysRevB.64.014411 PACS number(s): 75.30.Gw, 75.50.Cc, 75.60.Nt, 75.50.Ss

I. INTRODUCTION

In recent years, owing to the technological implications for high-density magneto-optical storage media,[1–4] there has been great interest in the magnetocrystalline anisotropy of ferromagnetic materials containing transition metals particularly in multilayered and thin film form. Areal densities of information storage systems are increasing continuously and are expected to reach 40 Gbits per square inch by the year 2004 requiring a grain size of less than 10 nm. For such applications the films and multilayers need to exhibit a very strong perpendicular magnetic anisotropy[5,6] (PMA) to avoid destabilization of the magnetization of recording bits by thermal fluctuations and demagnetizing fields.[7] Whereas in ultrathin films and multilayers the PMA is due to surface[8,9] and interface[10,11] effects, respectively, in thicker films of transition metal alloys it is the strong intrinsic bulk magnetocrystalline anisotropy which leads to PMA. Thick films of transition metal alloys are particularly interesting for magneto-optic recording because they are chemically stable and easy to manufacture. To design magnetic materials for future magneto-optic recording applications a detailed understanding of the mechanism of magnetocrystalline anisotropy is needed. A significant effort has been directed towards such an understanding from a first-principles electronic structure point of view but since magnetocrystalline anisotropy arises from spin-orbit coupling, essentially a relativistic effect,[12,13] a fully relativistic electronic structure framework is desirable.

Several experimental observations on ferromagnetic alloys indicate a correlation between compositional order and magnetocrystalline anisotropy in bulk samples[14–21] as well as in films.[22–35] Very recently,[36] we developed a ''first-principles'' theory of the interrelationship between magnetocrystalline anisotropy and atomic short-range order (ASRO). In this theory the electronic structure is treated within the spin-polarized fully relativistic Korringa-Kohn-Rostoker coherent-potential approximation[37] (SPR-KKR-CPA) and the compositional order is modeled using the framework of static concentration waves[38] and is an extension of our earlier work[39,40] on the magnetocrystalline anisotropy of disordered alloys. Within this scheme we showed that in a fcc-$Co_{0.5}Pt_{0.5}$ alloy ASRO has a profound influence on the magnetocrystalline anisotropy, especially in the way it disrupts cubic symmetry. In this paper, we describe our scheme in some detail and provide an in-depth study of this effect in some more transition metal alloys and also demonstrate the electronic origin of the enhancement of the magnetocrystalline anisotropy energy (MAE).

We have studied the effects of compositional modulation on the MAE of fcc-Co_cPt_{1-c} for $c=0.25$ and 0.5 alloys. Thick films of these alloys are potential magneto-optical recording materials because of their large perpendicular anisotropy,[22–26,41] large magneto-optic Kerr effect signals for a range of wavelengths (400–820 nm) compared to those from Co/Pt multilayers and TbFeCo films which are currently used,[22,23] suitable Curie temperatures[42] ($\sim$700 K), high oxidation and corrosion resistance as well as their chemical stability and ease of manufacture. We use our ASRO calculations to extrapolate to the observed ordered structures as well as some hitherto unfabricated structures of these alloys with same stoichiometry. This is pertinent now that it is possible to *tailor* compositionally modulated films to obtain better magneto-optic recording characteristics.[43,44]

We find that compositional ordering can enhance the size of MAE by some two orders of magnitude. Of particular interest is the case of $Co_{0.25}Pt_{0.75}$. The MAE for the perfect $L1_2$ ordered alloy is very small as in the homogeneously disordered alloy. However, breaking this symmetry by directional chemical order and creating *internal interfaces* greatly enhances the MAE, in agreement with the experimental observations.[33] By analyzing the electronic structure of these alloys we find that the electrons near the Fermi surface are largely responsible for the enhancement of MAE by compositional ordering.

Also, it is known experimentally that, upon ordering, the equiatomic CoPt alloy undergoes a modest tetragonal lattice distortion ($c/a=0.98$) which can also enhance the MAE. We have calculated the MAE of disordered fcc-$Co_{0.5}Pt_{0.5}$ alloy for different c/a ratios and find that this 2% tetragonalization would contribute only about 20% of the observed MAE. This is a clear indication that in CoPt system, the enhancement of MAE is primarily due to compositional order. This inference gets further credence from the fact that the fcc-$Co_{0.25}Pt_{0.75}$ alloy, which retains its cubic lattice structure upon ordering, also shows an enhancement of MAE when compositional order is introduced.

The $Fe_{0.5}Co_{0.5}$ alloy also has important magnetic properties, both from fundamental as well as a technological point of view. In this alloy, both the disordered phase as well as the ordered ($B2$) phase exhibit very low MAE and easy axes along the [111] direction.[45] Our calculations are in agreement with these experimental observations. This FeCo alloy is known to have a large linear magnetostriction.[45,46] By examining the MAE of this alloy under modest tetragonal lattice distortions we also investigate this feature.

Using the same theoretical framework, we have also studied another soft alloy and have looked at phenomenon of magnetic annealing in $Ni_{0.75}Fe_{0.25}$ permalloy, which develops uniaxial magnetic anisotropy when annealed in a magnetic field.[20,21] Because of its high permeability and low coercivity, permalloy is a good soft magnet and can be used for low switching fields in sensors. Also, a large difference in the conductivity of majority and minority spins[47] makes it a good candidate for spin-valves, spin transistors and magnetic tunnel junctions. On magnetic annealing, the permalloy develops directional chemical order[48,49] which is responsible for the uniaxial anisotropy. In the previous work[36] we showed from first-principles theoretical calculations that magnetic annealing can indeed produce directional chemical order. Here we isolate the electronic origin of the effect.

The outline of the paper is as follows. In Sec. II, we present the formulation and some numerical and technical details. Afterwards, we present our results in Sec. III and in Sec. IV we investigate the electronic origin of the MAE enhancement as well as of the magnetic annealing. Finally, in Sec. V we draw some conclusions.

II. FORMULATION

Our theory is based on the relativistic spin-polarized local density functional theory[50–52] and its solution by the SPR-KKR-CPA method.[37,53] A detailed description of the method for the homogeneously disordered ferromagnetic alloys is provided in Ref. 39, and will not be repeated. Here, we describe in detail our new framework to investigate the effects of ASRO on magnetocrystalline anisotropy (a brief summary of the approach has already been given in our recent letter Ref. 36). In Sec. II A we give a brief outline of the theory of compositional ordering within the SPR-KKR-CPA formalism and in Sec. II B we describe the scheme for studying the effects of ASRO on the MAE and show how this provides a theory of how directional compositional order can be induced into a magnetically soft alloy when it is annealed in a magnetic field. We also show how the calculations can be used to infer the MAE of ordered magnetic alloys.

A. Compositional order

We consider a binary alloy A_cB_{1-c} where the atoms are arranged on a fairly regular array of lattice sites. At high temperatures the alloy is homogeneously disordered and each site is occupied by an A- or B-type atom with probabilities c and $(1-c)$ respectively. Below some transition temperature, T_c, the system will either order or phase separate. A compositionally modulated alloy can be described by a set of site-occupation variables $\{\xi_i\}$, with $\xi_i=1(0)$ when the ith site in the lattice is occupied by an $A(B)$-type atom. The thermodynamic average, $\langle\xi_i\rangle$, of the site-occupation variable is the concentration c_i of an A-type atom at that site. At high temperatures where the alloy is homogeneously disordered, $c_i=c$ for all sites. When inhomogeneity sets in below T_c, the temperature-dependent inhomogeneous concentration fluctuations $\{\delta c_i\}=\{c_i-c\}$ can be written as a superposition of static concentration waves,[38] i.e.,

$$c_i=c+\frac{1}{2}\sum_{\mathbf{q}}\left[c_{\mathbf{q}}e^{i\mathbf{q}\cdot\mathbf{R}_i}+c_{\mathbf{q}}^{*}e^{-i\mathbf{q}\cdot\mathbf{R}_i}\right],$$

where $c_{\mathbf{q}}$ are the amplitudes of the concentration waves with wave vectors $\mathbf{q}$, and $\mathbf{R}_i$ are the lattice positions. Usually only a few concentration waves are needed to describe a particular ordered structure. For example, the CuAu-like $L1_0$ layered-ordered structure (Fig. 1) is set up by a single concentration wave with $c_{\mathbf{q}}=\frac{1}{2}$ and $\mathbf{q}=(001)$, the [111]-layered CuPt-like $L1_1$ ordered structure is set up by a concentration wave with $c_{\mathbf{q}}=\frac{1}{2}$ and $\mathbf{q}=(\frac{1}{2}\frac{1}{2}\frac{1}{2})$, and the Cu_3Au-like $L1_2$ ordered structure is set up by three concentration waves of identical amplitude $c_{\mathbf{q}}=\frac{1}{4}$ and wave vectors $\mathbf{q}_1=(100)$, $\mathbf{q}_2=(010)$, and $\mathbf{q}_3=(001)$ ($\mathbf{q}$ is in units of $2\pi/a$, a being the lattice parameter).

The grand potential for the interacting electrons in an inhomogeneous alloy with composition $\{c_i\}$ and magnetized along the direction $\mathbf{e}$ at a finite temperature T is given by[54–56]

$$\Omega(\{c_i\};\mathbf{e})=\nu Z-\int_{-\infty}^{\infty}d\varepsilon\, f(\varepsilon,\nu)N(\{c_i\},\varepsilon;\mathbf{e})+\Omega_{\mathrm{DC}}(\{c_i\};\mathbf{e}),\tag{2.1}$$

where, ν is the chemical potential, Z is the total valence charge, $f(\varepsilon,\nu)$ is the Fermi factor, $N(\{c_i\},\varepsilon;\mathbf{e})$ is the integrated electronic density of states, and $\Omega_{DC}(\{c_i\};\mathbf{e})$ is the ''double-counting'' correction to the grand potential.[55] The

derivatives of the grand potential with respect to the concentration variables give rise to a hierarchy of direct correlation functions. In particular, the second derivative evaluated at the equilibrium concentrations,

$$S^{(2)}_{jk}(\mathbf{e}) = -\left.\frac{\partial^2 \Omega(\{c_i\};\mathbf{e})}{\partial c_j \partial c_k}\right|_{\{c_i=c\}},$$

is the Ornstein-Zernike direct correlation function for our lattice model[54–58] (so called by the way of the close analogy with similar quantities defined for classical fluids[59,60]). These are related to the linear response functions, $\alpha_{ij}(\mathbf{e})$, through[56]

$$\left[1+\sum_k S^{(2)}_{ik}(\mathbf{e})\alpha_{ki}(\mathbf{e})\right]\alpha_{ij}(\mathbf{e}) = \beta c(1-c)\left[\delta_{ij}+\sum_k S^{(2)}_{ik}(\mathbf{e})\alpha_{kj}(\mathbf{e})\right], \quad (2.2)$$

where $\beta=(k_B T)^{-1}$, k_B being the Boltzmann constant. The linear response functions, $\alpha_{ij}(\mathbf{e})$, describe the resulting concentration fluctuations, $\{\delta c_i\}$, which are produced when a small inhomogeneous set of external chemical potentials, $\{\delta \nu_i\}$, is applied at all sites. Via the fluctuation dissipation theorem these are proportional to atomic pair-correlation functions, i.e., $\alpha_{ij}=\beta[\langle \xi_i \xi_j\rangle - \langle \xi_i\rangle\langle \xi_j\rangle]$). Upon taking the lattice Fourier transform of Eq. (2.2) we obtain a closed form of equations,[54–58]

$$\alpha(\mathbf{q},T;\mathbf{e}) = \frac{\beta c(1-c)}{1-\beta c(1-c)[S^{(2)}(\mathbf{q};\mathbf{e})-\Lambda_c(\mathbf{e})]}, \quad (2.3)$$

where, the Onsager cavity correction $\Lambda_c(\mathbf{e})$ is given by[56]

$$\Lambda_c(\mathbf{e}) = \frac{1}{\beta c(1-c)}\frac{1}{V_{\mathrm{BZ}}}\int d\mathbf{q}' S^{(2)}(\mathbf{q}';\mathbf{e})\alpha(\mathbf{q}',T;\mathbf{e}).$$

Here, $\alpha(\mathbf{q},T)$, the lattice Fourier transform of α_{ij}, are the Warren-Cowley ASRO parameters in the disordered phase. The Onsager cavity correction in Eq. (2.3) ensures that the spectral weight over the Brillouin zone is conserved,[56,58,61] so that, in other words, the diagonal part of the fluctuation dissipation theorem is honored, i.e., $\alpha_{ii}=\beta c(1-c)$.

The spinodal transition temperature T_c below which the alloy orders into a structure characterized by the concentration wave vector $\mathbf{q}_{\max}$ is determined by $S^{(2)}(\mathbf{q}_{\max};\mathbf{e})$, where $\mathbf{q}_{\max}$ is the value at which $S^{(2)}(\mathbf{q};\mathbf{e})$ is maximal. We can write[54,55]

$$T_c = \frac{c(1-c)[S^{(2)}(\mathbf{q}_{\max};\mathbf{e})-\Lambda_c(\mathbf{e})]}{k_B}.$$

The free energy for the disordered phase which is consistent with this description of ASRO can also be written down[62]

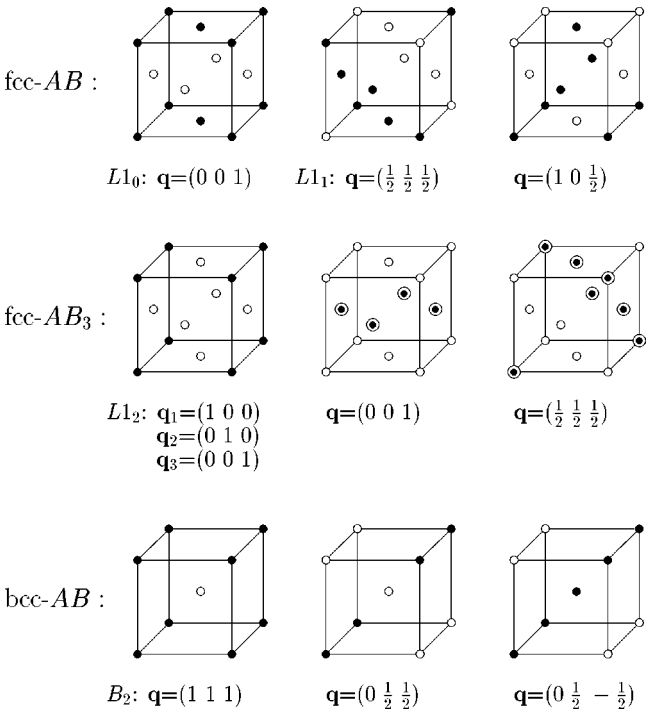

FIG. 1. Some ordered structures and their representative concentration wave vectors. For the AB-type stoichiometry $\mathbf{q}$=(001) and $\mathbf{q}$=($\frac{1}{2}\frac{1}{2}\frac{1}{2}$) generate respectively the CuAu-type $L1_0$ layered ordered structure with layers perpendicular to the [001] direction and the CuPt-type $L1_1$ layered-ordered structure with layers perpendicular to the [111] direction and $\mathbf{q}$=(10$\frac{1}{2}$) generates a layered structure with planes of an ordered structure of A and B atoms stacked along the [001] direction. For the AB_3-type composition, a combination of $\mathbf{q}_1$=(100), $\mathbf{q}_2$=(010), and $\mathbf{q}_3$=(001) generates the Cu_3Au-type $L1_2$ ordered structure. For this composition, a single wave vector $\mathbf{q}$=(001) generates a superstructure of alternating monolayers of pure B atoms and disordered $A_{0.5}B_{0.5}$ perpendicular to the [001] direction. Similarly, $\mathbf{q}$=($\frac{1}{2}\frac{1}{2}\frac{1}{2}$) generates a superstructure of monolayers of pure B atoms and disordered $A_{0.5}B_{0.5}$ perpendicular to the [111] direction. The full circles denote A atoms, open circles denote B atoms, and a full circle inscribed by an open circle denotes a CPA effective atom $A_{0.5}B_{0.5}$.

$$\mathcal{F}(\mathbf{e}) = \Omega(\{c_i=c\};\mathbf{e}) + \frac{1}{\beta}[c\ln c + (1-c)\ln(1-c)] - u\left(c-\frac{1}{2}\right) - \frac{1}{2}c(1-c)\Lambda_c(\mathbf{e}) + \frac{1}{2\beta}\frac{1}{V_{BZ}}\int d\mathbf{q}' \ln\{1-\beta c(1-c) \times [S^{(2)}(\mathbf{q}';\mathbf{e})-\Lambda_c(\mathbf{e})]\}. \quad (2.4)$$

The parameter u ensures that the number of $A(B)$ atoms in the alloy is conserved.

Within the SPR-KKR-CPA scheme, if we neglect charge rearrangement effects arising from compositional fluctuations[56] we obtain the following expression for $S^{(2)}_{jk}(\mathbf{e})$ from the Lloyd formula[63] for the integrated density of states in Eq. (2.1):

$$S_{jk}^{(2)}(\mathbf{e}) = -\frac{\mathrm{Im}}{\pi}\int_{-\infty}^{\infty} d\varepsilon\, f(\varepsilon,\nu)\mathrm{Tr}\Big[\{X^A(\mathbf{e})-X^B(\mathbf{e})\} \times \sum_{m\neq j}\tau^{jm}(\mathbf{e})\lambda^{mk}(\mathbf{e})\tau^{mj}(\mathbf{e})\Big], \tag{2.5}$$

where

$$X^{A(B)}(\mathbf{e}) = [\{t_{A(B)}^{-1}(\mathbf{e}) - t_c^{-1}(\mathbf{e})\}^{-1} + \tau^{00}(\mathbf{e})]^{-1}$$

and

$$\lambda^{jk}(\mathbf{e}) = \delta_{jk}\{X^A(\mathbf{e})-X^B(\mathbf{e})\} - X^A(\mathbf{e})\sum_{m\neq j}\tau^{jm}(\mathbf{e})\lambda^{mk}(\mathbf{e})\tau^{mj}(\mathbf{e})X^B(\mathbf{e}).$$

Here $t_{A(B)}(\mathbf{e})$ and $t_c(\mathbf{e})$ are the t matrices for electronic scattering from sites occupied by $A(B)$ atoms and CPA effective potentials respectively, and $\tau^{mj}(\mathbf{e})$ are the path operator matrices for the CPA effective medium in real space obtained by a lattice Fourier transform of $\tau(\mathbf{k};\mathbf{e})$, where

$$\tau(\mathbf{k};\mathbf{e}) = [t_c^{-1}(\mathbf{e}) - g(\mathbf{k})]^{-1},$$

$g(\mathbf{k})$ being the KKR structure constants matrix.[64] Now taking the lattice Fourier transform of Eq. (2.5), we get

$$S^{(2)}(\mathbf{q};\mathbf{e}) = -\frac{\mathrm{Im}}{\pi}\int_{-\infty}^{\infty} d\varepsilon\, f(\varepsilon,\nu) \times \sum_{L_1L_2L_3L_4}[\{X^A(\mathbf{e})-X^B(\mathbf{e})\}_{L_1L_2} \times I_{L_2L_3;L_4L_1}(\mathbf{q};\mathbf{e})\lambda_{L_3L_4}(\mathbf{q};\mathbf{e})], \tag{2.6}$$

where

$$\lambda_{L_1L_2}(\mathbf{q};\mathbf{e}) = \{X^A(\mathbf{e})-X^B(\mathbf{e})\}_{L_1L_2} - \sum_{L_3L_4L_5L_6}[X^A_{L_1L_5}(\mathbf{e})I_{L_5L_3;L_4L_6}(\mathbf{q};\mathbf{e}) \times X^B_{L_6L_2}(\mathbf{e})\lambda_{L_3L_4}(\mathbf{q};\mathbf{e})],$$

and

$$I_{L_5L_3;L_4L_6}(\mathbf{q};\mathbf{e}) = \frac{1}{V_{\mathrm{BZ}}}\int d\mathbf{k}\,\tau_{L_5L_3}(\mathbf{k}+\mathbf{q};\mathbf{e})\tau_{L_4L_6}(\mathbf{k};\mathbf{e}) - \tau^{00}_{L_5L_3}(\mathbf{e})\tau^{00}_{L_4L_6}(\mathbf{e}). \tag{2.7}$$

Experimentally, the instability of the disordered phase to ordering can be observed in diffuse electron, x-ray, or neutron scattering experiments. The experimentally measured intensities are proportional to the ASRO parameter. In previous work, the ASRO parameter $\alpha(\mathbf{q},T)$ and ordering temperature T_c have been calculated for many alloys, both nonmagnetic and ferromagnetic, and compared with diffuse x-ray and neutron scattering data.[55,56] However, in those studies, relativistic effects were largely ignored. These studies have revealed that the electronic structure around the Fermi level is sometimes the driving force behind unusual compositional ordering in some alloys.[54,56]

B. Magnetocrystalline anisotropy

The MAE of a compositionally disordered ferromagnetic alloy in the presence of ASRO can be evaluated from Eq. (2.4), $\Delta\mathcal{F}_{\mathrm{MAE}} = \mathcal{F}(\mathbf{e}_1) - \mathcal{F}(\mathbf{e}_2)$. This difference is small compared to the magnitude of $\mathcal{F}$ and can be written approximately as

$$\Delta\mathcal{F}_{\mathrm{MAE}} \approx [\Omega(\{c_i=c\};\mathbf{e}_1) - \Omega(\{c_i=c\};\mathbf{e}_2)] - \frac{1}{2\beta}\frac{1}{V_{\mathrm{BZ}}}\int d\mathbf{q}'\,\alpha(\mathbf{q}',T;\mathbf{e}_1) \times [S^{(2)}(\mathbf{q}';\mathbf{e}_1) - S^{(2)}(\mathbf{q}';\mathbf{e}_2)].$$

The first term describes the MAE of a randomly disordered alloy,[39] $K_{\mathrm{CPA}}(c)$, with the ASRO effects contained in the second term. When the alloy has significant ASRO $\alpha(\mathbf{q},T;\mathbf{e}_1)$ is a structured function of $\mathbf{q}$ with peaks located at $\mathbf{q}_{\max}$, wave vectors of the concentration waves which characterize the ordered phase the alloy can form at low temperatures at equilibrium. Now the second term becomes $\approx -\frac{1}{2}c(1-c)[S^{(2)}(\mathbf{q}_{\max};\mathbf{e}_1) - S^{(2)}(\mathbf{q}_{\max};\mathbf{e}_2)]$.

The MAE of alloys with long-ranged order can also be estimated from calculations of $S^{(2)}(\mathbf{q},\mathbf{e})$ as we now show. For an inhomogeneous alloy the MAE can be characterized by the change in the electronic grand-potential arising from the change in the magnetization direction. Thus

$$K(\{c_i\}) = \Omega(\{c_i\};\mathbf{e}_1) - \Omega(\{c_i\};\mathbf{e}_2),$$

where $\mathbf{e}_1$ and $\mathbf{e}_2$ are two magnetization directions. We assume that the double-counting correction $\Omega_{DC}(\{c_i\};\mathbf{e})$ is generally unaffected by the change in the magnetization direction, and therefore, only the first two terms of Eq. (2.1) contribute to the MAE,

$$K(\{c_i\}) = (\nu_1-\nu_2)Z - \int_{-\infty}^{\infty} d\varepsilon\, f(\varepsilon,\nu_1)N(\{c_i\},\varepsilon;\mathbf{e}_1) + \int_{-\infty}^{\infty} d\varepsilon\, f(\varepsilon,\nu_2)N(\{c_i\},\varepsilon;\mathbf{e}_2),$$

where ν_1 and ν_2 are the chemical potentials of the system when the magnetization is along $\mathbf{e}_1$ and $\mathbf{e}_2$ directions, respectively. The change in the chemical potential originates from a redistribution of the occupied energy bands in the Brillouin zone in the event of a change of magnetization direction. A Taylor expansion of $f(\varepsilon,\nu_2)$ about ν_1 and some algebra leads to

$$K(\{c_i\}) = \int_{-\infty}^{\infty} d\varepsilon\, f(\varepsilon,\nu_1)[N(\{c_i\},\varepsilon;\mathbf{e}_1) - N(\{c_i\},\varepsilon;\mathbf{e}_2)] + O(\nu_1-\nu_2)^2.$$

Note that the effect of the small change in the chemical potential on $K(\{c_i\})$ is of second order in $(\nu_1-\nu_2)$, and can be

shown to be very small compared to the first term.[39] We now expand $K(\{c_i\})$ around $K_{\mathrm{CPA}}(c)$, the MAE of the homogeneously disordered alloy A_cB_{1-c},

$$K(\{c_i\}) = K_{\mathrm{CPA}}(c) + \sum_j \left.\frac{\partial K(\{c_i\})}{\partial c_j}\right|_{\{c_i=c\}} \delta c_j + \frac{1}{2}\sum_{j,k} \left.\frac{\partial^2 K(\{c_i\})}{\partial c_j \partial c_k}\right|_{\{c_i=c\}} \delta c_j \delta c_k + O(\delta c)^3. \tag{2.8}$$

It is clear from Eq. (2.8) that we are considering only the effects of two-site correlations on the electronic grand potential and MAE. However, in principle it is possible to include higher order correlations, but computationally it will be prohibitive.

Within the SPR-KKR-CPA scheme, a formula for $K_{\mathrm{CPA}}(c)$ is obtained by using the Lloyd formula[63] for the integrated density of states,

$$K_{\mathrm{CPA}}(c) = -\frac{\mathrm{Im}}{\pi}\int_{-\infty}^{\infty} d\varepsilon\, f(\varepsilon,\nu_1)\left[\frac{1}{V_{\mathrm{BZ}}}\int d\mathbf{k} \times \ln\|I + \{t_c^{-1}(\mathbf{e}_2) - t_c^{-1}(\mathbf{e}_1)\}\tau(\mathbf{k};\mathbf{e}_1)\| + c(\ln\|D^A(\mathbf{e}_1)\| - \ln\|D^A(\mathbf{e}_2)\|) + (1-c) \times (\ln\|D^B(\mathbf{e}_1)\| - \ln\|D^B(\mathbf{e}_2)\|)\right] + \mathcal{O}(\nu_1-\nu_2)^2, \tag{2.9}$$

where

$$D^{A(B)}(\mathbf{e}) = [I + \tau^{00}(\mathbf{e})\{t_{A(B)}^{-1}(\mathbf{e}) - t_c^{-1}(\mathbf{e})\}]^{-1}.$$

Note that Eq. (2.9) is the finite temperature version of the expression of MAE of disordered alloys given in Ref. 39. Now, the variation of the MAE with respect to the change in the concentration variables is

$$\left.\frac{\partial K(\{c_i\})}{\partial c_j}\right|_{\{c_i=c\}} = -\frac{\mathrm{Im}}{\pi}\int_{-\infty}^{\infty} d\varepsilon\, f(\varepsilon,\nu_1) \times [\ln\|D^A(\mathbf{e}_1)\| - \ln\|D^B(\mathbf{e}_1)\| - \ln\|D^A(\mathbf{e}_2)\| + \ln\|D^B(\mathbf{e}_2)\|],$$

which is independent of the site index and so the second term in Eq. (2.8) vanishes if the number of A and B atoms in the alloy is to be conserved ($\Sigma_j \delta c_j = 0$). Also, we have

$$\left.\frac{\partial^2 K(\{c_i\})}{\partial c_j \partial c_k}\right|_{\{c_i=c\}} = -[S_{jk}^{(2)}(\mathbf{e}_1) - S_{jk}^{(2)}(\mathbf{e}_2)],$$

where $S_{jk}^{(2)}(\mathbf{e}_{1(2)})$ are the Ornstein-Zernike direct correlation functions[54] when the magnetization is along $\mathbf{e}_{1(2)}$. Now taking the Fourier transform of Eq. (2.8), we get the MAE of the compositionally modulated alloy with wave vector $\mathbf{q}$,

TABLE I. Direct correlation function $S^{(2)}(\mathbf{q};[001])$ for different $\mathbf{q}$ vectors for $Co_{0.25}Pt_{0.75}$ and $Fe_{0.5}Co_{0.5}$ alloys (the respective ordered structures are shown in Fig. 1).

Alloy	$\mathbf{q}$	Structure	$S^{(2)}(\mathbf{q};[001])$ (eV)	T_c (K)
	(100)	$L1_2$	0.43	935
	(010)	$L1_2$	0.43	935
$Co_{25}Pt_{75}$	(001)	$L1_2$	0.43	935
	$(\frac{1}{2}\frac{1}{2}\frac{1}{2})$		0.22	
	$(1\frac{1}{2}0)$	DO_{22}	0.19	
	$(\frac{1}{2}01)$	DO_{22}	0.19	
	(100)	$B2$	0.44	1286
$Fe_{50}Co_{50}$	(001)	$B2$	0.44	1286
	(111)	$B2$	0.44	1286
	$(\frac{1}{2}\frac{1}{2}0)$		0.02	

$$K(\mathbf{q}) = K_{\mathrm{CPA}}(c) + \frac{1}{2}|c_{\mathbf{q}}|^2 K^{(2)}(\mathbf{q}), \tag{2.10}$$

where

$$K^{(2)}(\mathbf{q}) = -[S^{(2)}(\mathbf{q};\mathbf{e}_1) - S^{(2)}(\mathbf{q};\mathbf{e}_2)]. \tag{2.11}$$

Equation (2.10) thus shows a direct relationship between the type of compositional modulation and the MAE. Also, by calculating $S^{(2)}(\mathbf{q};\mathbf{e})$ for different $\mathbf{q}$ vectors, while keeping the magnetic field and magnetization direction fixed, one can study the effect of an applied magnetic field on the compositional modulation of a solid solution, and thus can describe the phenomenon of magnetic annealing. In this case, the $\mathbf{q}$ vector for which $S^{(2)}(\mathbf{q};\mathbf{e})$ is maximal will represent the compositional modulation induced in the alloy when it is annealed in the magnetic field.

The technical and computational details are discussed in Refs. 36 and 39. The convolution integral given by Eq. (2.7) is evaluated using the adaptive grid method[65] with a relative accuracy $\epsilon = 10^{-6}$, which means that the values of $S^{(2)}(\mathbf{q};\mathbf{e})$ and $K(\mathbf{q})$ are accurate to within 0.1 μeV.

III. RESULTS AND DISCUSSION

A. $Co_{50}Pt_{50}$ and $Co_{25}Pt_{75}$ alloys

We have studied Co_cPt_{1-c} alloys for $c = 0.5$ and 0.25. The results for $Co_{0.5}Pt_{0.5}$ alloy were presented in our previous publication,[36] where we showed that compositional order enhances the MAE by some two orders of magnitude. In particular, our calculated value of the MAE of the $L1_0$ ordered structure (58.6 μeV) is comparable to the experimental value[14–16] ($\sim$130 μeV) as well as to the calculated value of the $L1_0$-ordered tetragonal CoPt alloy.[67] Also, we predicted that the [111]-layered $L1_1$ structure will have a larger MAE than that of a $L1_0$ ordered structure. This is confirmed by recent experiments.[68,69] Recent first-principles theoretical calculations[70,71] of the MAE of superstructures of CoPt on Pt(001) and Pt(111) substrates also are in agreement with our results.

TABLE II. Magnetocrystalline anisotropy energy $K(\mathbf{q})$ for several compositionally modulated $Co_{0.25}Pt_{0.75}$ alloys characterized by different $\mathbf{q}$ vectors (the respective ordered structures are shown in Fig. 1). Here $K(\mathbf{q})$ are calculated with respect to the reference system which has the magnetization along the [001] direction (i.e., $\mathbf{e_1}=[001]$) of the crystal. Thus, when $K(\mathbf{q})<0$ the easy axis is along [001] and when $K(\mathbf{q})>0$ the easy axis is along $\mathbf{e}_2$.

$\mathbf{q}$	Structure	$K(\mathbf{q})$ (μeV)		Easy axis
		$\mathbf{e}_2=[111]$	$\mathbf{e}_2=[100]$	
(100)	[100]-Layered	−29.0	−83.6	[001]
(010)	[010]-Layered	−29.0	0.0	
(001)	[001]-Layered	54.6	83.6	[100]
(100),(010),(001)	$L1_2$	−3.4	0.0	[001]
$(1\frac{1}{2}0)$		54.0	0.0	[111]
$(10\frac{1}{2})$		−98.6	−152.5	[001]

The results for $Co_{0.25}Pt_{0.75}$ are presented in Tables I and II. Our calculated value of $S^{(2)}(\mathbf{q})$ has maxima for $\mathbf{q}=(100)$, (010), and (001) implying that a $L1_2$ ordered structure is favored with a transition temperature of 935 K in excellent agreement with the experimental value of 960 K (Ref. 72). Note that, a combination of three wave vectors $\mathbf{q}_1=(100)$, $\mathbf{q}_2=(010)$, and $\mathbf{q}_3=(001)$ generates the isotropic $L1_2$ ordering, while a single wave vector, for example, $\mathbf{q}_1=(001)$ generates a layered structure with directional compositional ordering along the [001] direction. This is a superstructure consisting of alternating monolayers of pure Pt and $Co_{0.5}Pt_{0.5}$, as depicted in Fig. 1. In this structure, therefore, there are no out-of-plane Co-Co bonds, only in-plane Co-Co bonds which can produce in-plane Co-Co nearest neighbor pairs. We find that for this structure the MAE is quite large (~84 μeV). In a recent experiment,[28] it was found that the [001]-textured thick films of $Co_{0.25}Pt_{0.75}$ alloy deposited at 670 K do have this type of structure, i.e., there are stacks of Pt and $Co_{0.5}Pt_{0.5}$ monolayers perpendicular to the [001] direction, and these films exhibit PMA. It should be emphasized, however, for the perfect $L1_2$ structure, where all the three wave vectors, namely, $\mathbf{q}_1=(100)$, $\mathbf{q}_2=(010)$, and $\mathbf{q}_3=(001)$ contribute, the MAE is very small, comparable to that of the disordered alloy. We are not aware of any experimental results on the bulk ordered $Co_{0.25}Pt_{0.75}$ system. However, it is reported that [111]-textured thick films grown around 690 K having anisotropic compositional order exhibit large uniaxial anisotropy,[24,25,34] whereas films deposited around 800 K with a $L1_2$-type isotropic chemical order exhibit no anisotropy. These observations are clearly in good agreement with our results.

It is well known that disordered fcc-$Co_{0.5}Pt_{0.5}$ undergoes a phase transformation into a CuAu-type $L1_0$ ordered tetragonal structure[14,66] with a c/a ratio of 0.98 and $Co_{0.25}Pt_{0.75}$ orders into a Cu_3Au-type $L1_2$ cubic structure.[72] Thus, in $Co_{0.5}Pt_{0.5}$, there is a tetragonalization of the lattice which also lowers the symmetry and contributes to MAE enhancement, whereas in $Co_{0.25}Pt_{0.75}$ there is no such additional effect, owing to the lattice remaining cubic even in the ordered phase. With this in mind we have calculated the MAE of disordered volume-conserving face-centered-tetragonal $Co_{0.5}Pt_{0.5}$ alloy as a function of the c/a ratio. The results are presented in Fig. 2. We point out that in these calculations we have used the atomic-sphere approximation for the single-site potentials and that the potentials and the Fermi energy are those of the disordered fcc-$Co_{0.5}Pt_{0.5}$ alloy. To estimate the magnitude of the effect of tetragonalization we have ''frozen'' these potentials as the c/a ratio has been altered. We observe that the MAE is a monotonically decreasing function of the c/a ratio, and that it is positive for $c/a<1.0$ and negative for $c/a>1.0$. This is consistent with the experimental observations that the magnetostriction constant, Λ_{001}, is positive[32,73] for the disordered $Co_{0.5}Pt_{0.5}$ alloy, because, as shown by, e.g., Freeman *et al.*[74], Λ_{001} is proportional to the rate of change of MAE with respect to the c/a ratio with opposite sign (note that, there is a sign difference in our definition of MAE and that of Freeman *et al.*). Therefore, our results are in qualitative agreement with the experimental observations. The MAE at the experimental value of c/a (0.98) is about 25 μeV which is less than 20% of the experimentally observed MAE. Most importantly, the sign of MAE for a tetragonally distorted compositionally disordered $Co_{0.5}Pt_{0.5}$ with this value of c/a is positive which means that the magnetic easy axis is not along the [001] direction (c-axis) in direct contradiction to the experimental observations. Consequently, we conclude that in the ordered alloys of Co and Pt lattice distortion is not the major factor in enhancing the MAE rather it is the compositional order which is primarily responsible for the large MAE.

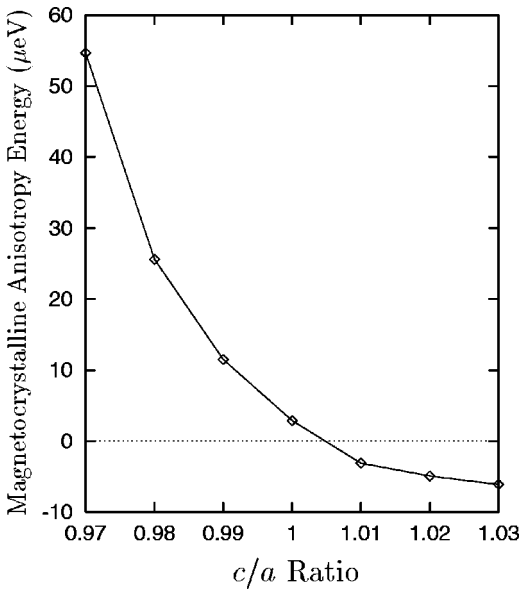

FIG. 2. Magnetocrystalline anisotropy energy (MAE) of disordered volume-conserving face-centered tetragonal (fct) $Co_{0.5}Pt_{0.5}$ alloy as a function of the c/a ratio.

B. $Fe_{0.5}Co_{0.5}$ alloy

FeCo alloys exhibit high saturation magnetizations, low magnetocrystalline anisotropies, and high Curie temperatures, and therefore are potential candidates for high temperature magnets in such applications as rotors in electric

TABLE III. Magnetocrystalline anisotropy energy $K(\mathbf{q})$ for several compositionally modulated $Fe_{0.5}Co_{0.5}$ alloys characterized by different $\mathbf{q}$ vectors (the respective ordered structures are shown in Fig. 1). Here $K(\mathbf{q})$ are calculated with respect to the reference system which has the magnetization along the [001] direction (i.e., $\mathbf{e_1}=[001]$) of the crystal. Thus, when $K(\mathbf{q})<0$ the easy axis is along [001] and when $K(\mathbf{q})>0$ the easy axis is along $\mathbf{e}_2$.

$\mathbf{q}$	Structure	$K(\mathbf{q})$ (μeV)		Easy axis
		$\mathbf{e}_2=[111]$	$\mathbf{e}_2=[100]$	
(100)	$B2$	−0.2	0.0	[001]
(001)	$B2$	−0.2	0.0	[001]
(111)	$B2$	−0.2	0.0	[001]
$(\frac{1}{2}\frac{1}{2}0)$		12.0		[111]
$(-\frac{1}{2}\frac{1}{2}0)$		−94.6		[001]
$(\frac{1}{2}0\frac{1}{2})$		74.8		[111]
$(-\frac{1}{2}0\frac{1}{2})$		−31.9		[001]

aircraft engines.[75,76] The bcc disordered $Fe_{0.5}Co_{0.5}$ alloy undergoes a phase transition to an ordered $B2$ structure[76,45] below 1000 K, and both the ordered as well as the disordered phases have a very low magnetocrystalline anisotropy but somewhat large magnetostriction.[45,46] The experimental value[45] of the MAE $[E(001)-E(111)]$ for the disordered phase is less than 1.0 μeV per atom with the easy axis is along the [111] direction of the crystal and for the $B2$ ordered phase the MAE is almost zero. Our results are summarized in Tables I and III. Our calculated value of the order-disorder transition temperature (1286 K) is comparable to the experimental value of 1000 K. The agreement is quite good considering that ours is a mean-field approach. Also there is good agreement between the calculated value of MAE of the disordered phase ($K_{\mathrm{CPA}}=0.3$ μeV) and the experimental value (it is difficult to compare the absolute values of the theoretical and experimental values of MAE, because, those are of the order of 0.1 μeV, which is the accuracy of our calculations). Nevertheless, we predict the correct easy axis for the disordered phase. For the B_2 ordered phase, the $K^{(2)}(\mathbf{q})$ [for $\mathbf{q}=(100)$, (010), (001), and (111)] is negative while the absolute value is comparable to K_{CPA}. Therefore, the MAE of the B_2 phase is even smaller than that of the disordered phase, in good agreement with experiment. Here again, we emphasize the role of symmetry and layer stacking in the determination of the easy magnetization axis. Note that $\mathbf{q}=(100)$, $\mathbf{q}=(010)$, $\mathbf{q}=(001)$, as well as $\mathbf{q}=(111)$, generate the same $B2$ structure, unlike the case in a fcc lattice. Our calculation does show that the results are also identical. This is an indicator of the accuracy and robustness of our computational procedure. Since the B_2 structure, unlike the $L1_0$ structure in the fcc lattice, has cubic symmetry, the ordering in this case does not enhance the magnitude of the MAE. The easy axis for this structure seems to be along one of the [100] axes. We have also calculated the MAE for some hypothetical structures shown in Fig. 1. These structures do not seem to be layered structures, however, the MAE of some of these structures is some two orders of magnitude larger than the equilibrium ordered structure as well as the disordered phase.

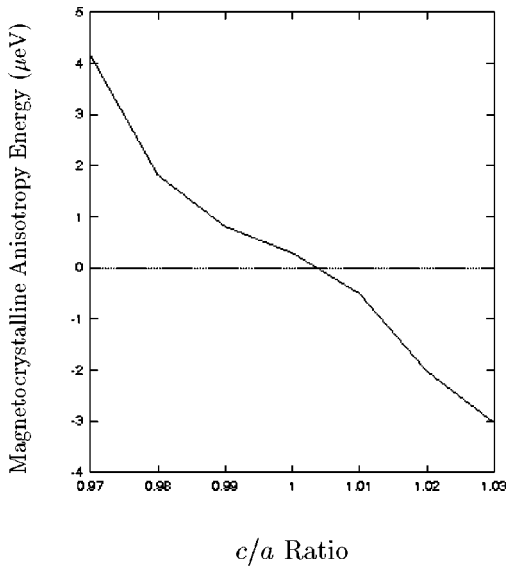

FIG. 3. Magnetocrystalline anisotropy energy (MAE) of disordered volume-conserving body-centered tetragonal (bct) $Fe_{0.5}Co_{0.5}$ alloy as a function of the c/a ratio.

We have also studied the effect of tetragonalization of the lattice on the MAE of the disordered $Fe_{0.5}Co_{0.5}$ alloy. The calculations are similar to those for the $Co_{0.5}Pt_{0.5}$ alloy discussed in the previous section. We show the MAE as a function of the c/a ratio in Fig. 3. In this case we observe that lattice distortion enhances the MAE slightly. The slope of the MAE versus the c/a ratio curve is negative implying that the alloy has a positive magnetostriction constant consistent with the experimental observations.[45] Assuming the total energy of the system to be a quadratic function of $\delta=c/a-1$, the tetragonal distortion, i.e., $E=E_0+a\delta+b\delta^2$, it can be shown[74] that the magnetostriction constant is proportional to the ratio of the δ-rate of change of MAE to the elastic constant b. Evidently the fairly moderate value of the former indicates that the large linear magnetostriction of this alloy must be linked directly to the softness of the latter. We note that the average number of valence electrons per atom in this alloy is close to that in the famous NiFe invar alloys and consequently we are planning a study of b as a function of c for Fe_cCo_{1-c} alloys.

Another soft magnetic alloy, permalloy $Ni_{0.75}Fe_{0.25}$ orders into a $L1_2$ structure[77] below 820 K in which phase it retains its soft magnetic properties. However at this stoichiometry when annealed in a magnetic field, this alloy can develop a significant uniaxial magnetic anisotropy depending on the direction of the applied field with respect to the crystallographic axes.[20,21] This phenomenon can be interpreted in terms of the creation of directional chemical order in the material.[48,49] A recent study based on magneto-optic Kerr effect measurements[78] also reveals that magnetic annealing can induce uniaxial anisotropy. Previous studies based on nonrelativistic electronic structure calculations[79] and Monte Carlo simulations[80] have shown that in this system compositional and magnetic ordering have a large influence on each other. However, to describe magnetic annealing a fully relativistic treatment is needed. In Ref. 36, we produced the first

quantitative description of magnetic annealing from *ab initio* electronic structure calculations in $Ni_{0.75}Fe_{0.25}$. We found that ordering is favored along the direction of the applied field.

IV. ELECTRONIC ORIGIN OF MAGNETIC ANISOTROPY

In elemental solids and the disordered alloys the MAE originates from a redistribution of electronic states around the Fermi level caused by the change in the magnetization direction.[39] The electronic structure of the disordered phase around the Fermi level is also partly responsible for the tendency to compositional order in some alloys.[54,56] We expect therefore that the enhancement of MAE in the compositionally modulated alloys is also related to this aspect of the disordered phase's electronic structure and demonstrate it in this section.

First we consider the electronic mechanism underlying the compositional ordering tendency. As presented in Table I, our calculation predicts $L1_0$-type order in $Co_{0.5}Pt_{0.5}$ which is in excellent agreement with experiment. The quantity $S^{(2)}(\mathbf{q};\mathbf{e})$ given by Eq. (2.6) can be rewritten as

$$S^{(2)}(\mathbf{q};\mathbf{e}) = -\frac{\mathrm{Im}}{\pi}\int_{-\infty}^{\infty} d\varepsilon\, f(\varepsilon,\nu) F(\mathbf{q},\varepsilon;\mathbf{e}),$$

where

$$F(\mathbf{q},\varepsilon;\mathbf{e}) = \sum_{L_1L_2L_3L_4} [\{X^A(\mathbf{e}) - X^B(\mathbf{e})\}_{L_1L_2} \times I_{L_2L_3;L_4L_1}(\mathbf{q};\mathbf{e}) \lambda_{L_3L_4}(\mathbf{q};\mathbf{e})]. \quad (4.1)$$

$S^{(2)}(\mathbf{q})$ is an integrated quantity and can also be written in terms of a sum[81] over Matsubara frequencies,[82] $\omega_n = (2n+1)\pi k_B T$,

$$S^{(2)}(\mathbf{q};\mathbf{e}) = 2k_B T \sum_n \mathrm{Re}[F(\mathbf{q},\nu + i\omega_n;\mathbf{e})].$$

In Fig. 4 we show a plot of $F(\mathbf{q},\varepsilon;[001])$ calculated for energies along the imaginary axis perpendicular to the Fermi level for $\mathbf{q}$ vectors (000), (001), $(\frac{1}{2}\frac{1}{2}\frac{1}{2})$ and $(10\frac{1}{2})$. The area under these curves is indicative of the strength of $S^{(2)}(\mathbf{q};[001])$ for these $\mathbf{q}$ vectors and is obviously greatest for $\mathbf{q}=(100)$.

Now we discuss the interplay between MAE and compositional order. Again, the quantity $K^{(2)}(\mathbf{q})$ given by Eq. (2.11) is an integrated quantity which can be written as a sum of contributions evaluated at the Matsubara frequencies,[81]

$$K^{(2)}(\mathbf{q}) = \frac{\mathrm{Im}}{\pi}\int_{-\infty}^{\infty} d\varepsilon\, f(\varepsilon,\nu)\Delta F(\mathbf{q},\varepsilon)$$

$$= -2k_B T \sum_n \mathrm{Re}[\Delta F(\mathbf{q},\nu + i\omega_n)], \quad (4.2)$$

where

$$\Delta F(\mathbf{q},\varepsilon) = F(\mathbf{q},\varepsilon;\mathbf{e}_1) - F(\mathbf{q},\varepsilon;\mathbf{e}_2). \quad (4.3)$$

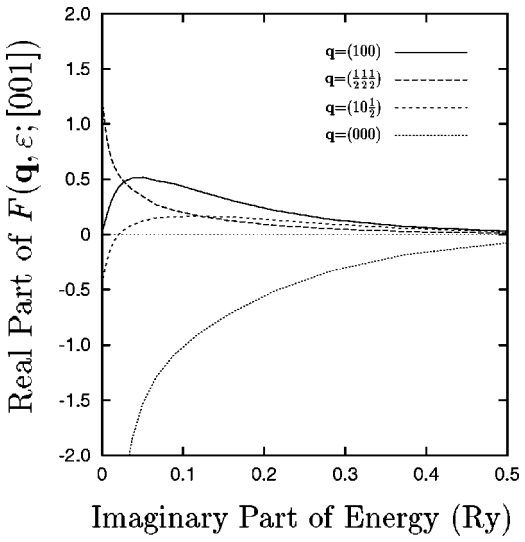

FIG. 4. Real part of $F(\mathbf{q},\varepsilon,[001])$, as given by Eq. (4.1), for $\mathbf{q}=(100)$ (full line), $(\frac{1}{2}\frac{1}{2}\frac{1}{2})$ (long-dashed line), $(10\frac{1}{2})$ (short-dashed line), and (000) (dotted line) at complex energies along the imaginary axis perpendicular to the Fermi level for disordered $Co_{0.5}Pt_{0.5}$ alloy.

In Fig. 5 we show a plot of $\Delta F(\mathbf{q},\varepsilon)$ with $\mathbf{e}_1=[001]$ and $\mathbf{e}_2=[111]$ calculated for energies along the imaginary axis perpendicular to the Fermi level for $\mathbf{q}$ vectors (000), (001), $(\frac{1}{2}\frac{1}{2}\frac{1}{2})$ and $(10\frac{1}{2})$. The area under these curves is indicative of the magnitude of $K^{(2)}(\mathbf{q})$ for these $\mathbf{q}$ vectors. The striking feature is that, unlike Fig. 4, the principal contributions for most $\mathbf{q}$ vectors are near the real axis indicating that the Fermi surface plays the dominant role in the enhancement of the MAE as well as the direction of easy magnetization. This can be illustrated more convincingly if one calculates $\Delta F(\mathbf{q},\varepsilon)$

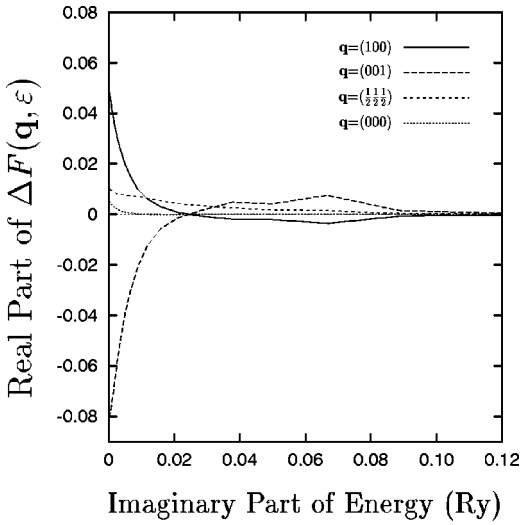

FIG. 5. Real part of $\Delta F(\mathbf{q},\varepsilon)$, as defined in Eq. (4.3), with $\mathbf{e}_1=[001]$ and $\mathbf{e}_2=[111]$ for $\mathbf{q}=(100)$ (full line), (001) (long-dashed line), $(\frac{1}{2}\frac{1}{2}\frac{1}{2})$ (short-dashed line), and (000) (dotted line) at complex energies along the imaginary axis perpendicular to the Fermi level for $Co_{0.5}Pt_{0.5}$ alloy. Note the different scales on the *x* and *y* axes of this figure and Fig. 4.

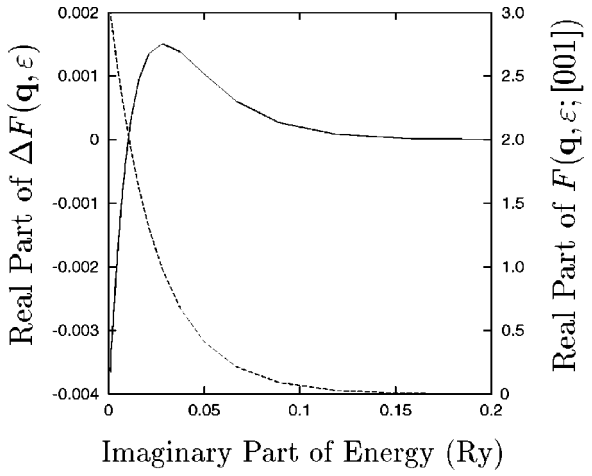

FIG. 6. Real part of $\Delta F(\mathbf{q},\varepsilon)$ as defined in Eq. (4.3) with $\mathbf{e}_1=[001]$ and $\mathbf{e}_2=[100]$ (full line, left scale) and real part of $F(\mathbf{q},\varepsilon;[001])$, as defined in Eq. (4.1) for $\mathbf{q}=(001)$ (dashed line, right scale) at complex energies along the imaginary axis perpendicular to the Fermi level for $Ni_{0.75}Fe_{0.25}$ alloy.

for a range of energies just above the real axis. But since calculation of $\Delta F(\mathbf{q},\varepsilon)$ for energies close to real axis is extremely demanding,[36] we continue analytically the values of $\Delta F(\mathbf{q},\varepsilon)$ for complex energies to the energies just above the real axis. In order to achieve this, we first fit our data to a rational function,

$$\Delta F(\mathbf{q},\varepsilon)=U(\mathbf{q})\frac{1+\sum_{k=1}^{M-2}a_k(\mathbf{q})\varepsilon^k}{1+\sum_{k=1}^{M}b_k(\mathbf{q})\varepsilon^k}.$$

The choice of the rational function ensures that $\lim_{\varepsilon\to\infty}\Delta F(\mathbf{q},\varepsilon)\sim 1/\varepsilon^2$ as indicated by Eqs. (2.6), (2.7), and (2.11). We find that very good fits are obtained with reasonably small M. We have calculated the imaginary part of $\Delta F(\mathbf{q},\varepsilon)$ for real energies by the above procedure, and find that except for $\mathbf{q}=(\frac{1}{2}\frac{1}{2}\frac{1}{2})$ which has a long tail extending beyond 0.1 Ry below the Fermi energy, most of the contributions to MAE come from electrons in a very narrow region below the Fermi energy. This corroborates the above idea that the electrons around the Fermi surface play a major role in the enhancement of the MAE as well as the direction of easy magnetization.

Now we discuss the electronic origin of magnetic annealing effect in $Ni_{0.75}Fe_{0.25}$ alloy. The difference between $S^{(2)}(\mathbf{q};[001])$ and $S^{(2)}(\mathbf{q};[100])$ for different $\mathbf{q}$ vectors is quite small; it is large enough to be observed by diffuse x-ray, electron, and neutron scattering experiments. Because of the small difference in these quantities, in Fig. 6 we plot the real part of $\Delta F(\mathbf{q},\varepsilon)$ which is related to the difference between $S^{(2)}(\mathbf{q};[001])$ and $S^{(2)}(\mathbf{q};[100])$ for $\mathbf{q}=(001)$ for energies along the imaginary axis perpendicular to the Fermi level (left-hand scale). We also plot $F(\mathbf{q},\varepsilon;[001])$ which is related to $S^{(2)}(\mathbf{q};[001])$ for $\mathbf{q}=(001)$ for the same energies (right-hand scale). We note that, these two quantities peak near the Fermi energy, i.e., when the imaginary part of the energy is very small. This is an indication that this process is also governed by the electrons near the Fermi surface.

V. CONCLUSIONS

We have presented the details of our *ab initio* theory of the connection between magnetocrystalline anisotropy of ferromagnetic alloys and compositional order within the SPR-KKR-CPA scheme. This theory has been applied to fcc-Co_cPt_{1-c} alloys. We found that when cooled from a high temperature, fcc-$Co_{0.5}Pt_{0.5}$ tends to order into an $L1_0$ layered-ordered structure around 1360 K and fcc-$Co_{0.25}Pt_{0.75}$ tends to order into $L1_2$ structure around 935 K, in good agreement with experimental observations. Also, we found that in $L1_0$ ordered CoPt the magnitude of the MAE is enhanced with the [111]-stacked CuPt-like $L1_1$ structure having the largest MAE. By examining the dependence of the MAE upon lattice tetragonalization we have been able to confirm that the MAE enhancement in the ordered alloy is primarily due to compositional factors. In the $L1_2$ ordered $CoPt_3$ the MAE is very small comparable to that of its disordered counterpart. However, in case of directional ordering along any of the [100], [010] or [001] directions the MAE is greatly enhanced. By analyzing the electronic structure of the disordered alloys near the Fermi energy we have found that the Fermi surface plays the dominant role in the enhancement of MAE. We have also carried out a study of the MAE of another alloy bcc-$Fe_{50}Co_{50}$ and have shown the MAE of this magnetically soft alloy to be little affected by both compositional order and lattice distortion. Finally within the same theoretical framework we explain the appearance of directional chemical order in another magnetically soft alloy, permalloy, $Ni_{0.75}Fe_{0.25}$ when it is annealed in an applied magnetic field and linked that also to the alloy's Fermi surface. As a last remark, we look forward to future work in which the effects of compositional structure are fully incorporated into micromagnetic modeling of transition metallic materials via *ab initio* electronic structure calculations.

ACKNOWLEDGMENTS

We thank B. L. Gyorffy and G. A. Gehring for helpful discussions. This research was supported by the Engineering and Physical Sciences Research Council (UK), National Science Foundation (USA), and the Training and Mobility of Researchers Network on ''Electronic structure calculation of materials properties and processes for industry and basic sciences.'' We also thank the Computing Services for Academic Research (CSAR) at Manchester University as part of the calculations were performed on their Cray T3E machine.

[1] L. M. Falicov, D. T. Pierce, S. D. Bader, R. Gronsky, K. H. Hathaway, H. J. Hopster, D. N. Lambeth, S. P. Parkin, G. Prinz, M. Salamon, I. K. Schuller, and R. H. Victora, J. Mater. Res. **5**, 1299 (1990).
[2] T. Wakiyama, in *Physics and Engineering Applications of Magnetism*, edited by Y. Ishikawa and N. Miura (Springer-Verlag, Berlin, 1991), p.133.
[3] B. Heinrich and J. F. Cochran, Adv. Phys. **42**, 523 (1993).
[4] M. T. Johnson, P. J. H. Bloemen, F. J. A. den Broeder, and J. J. de Vries, Rep. Prog. Phys. **59**, 1409 (1996).
[5] M. H. Kryder, W. Messner, and L. R. Carley, J. Appl. Phys. **79**, 4485 (1996).
[6] D. N. Lambeth, E. M. T. Velu, G. H. Bellesis, L. L. Lee, and D. E. Laughlin, J. Appl. Phys. **79**, 4496 (1996).
[7] C. Tsan, M. M. Chen, and T. Yogi, Proc. IEEE **81**, 1344 (1993).
[8] X. Le Cann, C. Boeglin, B. Carriére, and K. Hricovini, Phys. Rev. B **54**, 373 (1996).
[9] H. A. Dürr, G. van der Laan, J. Lee, G. Lauhoff, and J. A. C. Bland, Science **277**, 213 (1997).
[10] G. H. O. Daalderop, P. J. Kelly, and F. J. A. den Broeder, Phys. Rev. Lett. **68**, 682 (1992).
[11] P. Bruno, Phys. Rev. B **39**, 865 (1989).
[12] H. Brooks, Phys. Rev. **58**, B909 (1940).
[13] H. J. F. Jansen, Phys. Rev. B **38**, 8022 (1988).
[14] G. Hadjipanayis and P. Gaunt, J. Appl. Phys. **50**, 2358 (1979).
[15] B. Zhang and W. A. Soffa, Scr. Metall. Mater. **30**, 683 (1994).
[16] R. A. McCurrie and P. Gaunt, Philos. Mag. **13**, 567 (1966); P. Gaunt, *ibid.* **13**, 579 (1966).
[17] N. Miyata, K. Tomotsune, H. Nakada, M. Hagiwara, H. Kadomatsu, and H. Fujiwara, J. Phys. Soc. Jpn. **55**, 946 (1986).
[18] N. Miyata, M. Hagiwara, H. Kunitomo, S. Ohishi, Y. Ichiyanagi, K. Kuwahara, K. Tsuru, H. Kadomatsu, and H. Fujiwara, J. Phys. Soc. Jpn. **55**, 953 (1986).
[19] N. Miyata, H. Asami, T. Mizushima, and K. Sato, J. Phys. Soc. Jpn. **59**, 1817 (1990).
[20] S. Chikazumi, J. Phys. Soc. Jpn. **11**, 551 (1956).
[21] E. T. Ferguson, J. Appl. Phys. **29**, 252 (1958).
[22] D. Weller, H. Brändle, G. Gorman, C.-J. Lin, and H. Notarys, Appl. Phys. Lett. **61**, 2726 (1992).
[23] D. Weller, H. Brändle, and C. Chapert, J. Magn. Magn. Mater. **121**, 461 (1993).
[24] M. Maret, M. C. Cadeville, R. Poinsot, A. Herr, E. Beaurepair, and C. Monier, J. Magn. Magn. Mater. **166**, 45 (1997).
[25] M. Maret, M. C. Cadeville, W. Staiger, E. Beaurepair, R. Poinsot, and A. Herr, Thin Solid Films **275**, 224 (1996).
[26] W. Grange, M. Maret, J.-P. Kappler, J. Vogel, A. Fontaine, F. Petroff, G. Krill, A. Rogalev, J. Goulon, M. Finazzi, and N. B. Brooks, Phys. Rev. B **58**, 6298 (1998).
[27] W. Grange, J. P. Kappler, M. Maret, J. Vogel, A. Fontaine, F. Petroff, G. Krill, A. Rogalev, J. Goulon, M. Finazzi, and N. Brookes, J. Appl. Phys. **83**, 6617 (1998).
[28] S. Iwata, S. Yamashita, and S. Tsunashima, IEEE Trans. Magn. **MAG-33**, 3670 (1997).
[29] S. Iwata, S. Yamashita, and S. Tsunashima, J. Magn. Magn. Mater. **198-199**, 381 (1999).
[30] G. R. Harp, D. Weller, T. A. Rabedeau, R. F. C. Farrow, and M. F. Toney, Phys. Rev. Lett. **71**, 2493 (1993).
[31] Y. Yamada, T. Suzuki, and E. N. Abarra, IEEE Trans. Magn. **MAG-34**, 343 (1998).
[32] S. Hashimoto, Y. Ochiai, and K. Aso, J. Appl. Phys. **66**, 4909 (1989).
[33] T. A. Tyson, S. D. Conradson, R. F. C. Farrow, and B. A. Jones, Phys. Rev. B **54**, 3702 (1996).
[34] P. W. Rooney, A. L. Shapiro, M. Q. Tran, and F. Hellman, Phys. Rev. Lett. **75**, 1843 (1995).
[35] P. Kamp, A. Marty, B. Gilles, R. Hoffmann, S. Marchesini, M. Belakhovsky, C. Boeglin, H. A. Dürr, S. S. Dhesi, G. van der Laan, and A. Rogalev, Phys. Rev. B **59**, 1105 (1999).
[36] S. S. A. Razee, J. B. Staunton, B. Ginatempo, F. J. Pinski, and E. Bruno, Phys. Rev. Lett. **82**, 5369 (1999).
[37] H. Ebert, B. Drittler, and H. Akai, J. Magn. Magn. Mater. **104-107**, 733 (1992).
[38] A. G. Khachaturyan, *Theory of Structural Transformations in Solids* (Wiley, New York, 1983), p. 39.
[39] S. S. A. Razee, J. B. Staunton, and F. J. Pinski, Phys. Rev. B **56**, 8082 (1997).
[40] S. S. A. Razee, J. B. Staunton, F. J. Pinski, B. Ginatempo, and E. Bruno, J. Appl. Phys. **83**, 7097 (1998).
[41] C. J. Lin and G. L. Gorman, Appl. Phys. Lett. **61**, 1600 (1992).
[42] D. Treves, J. T. Jacobs, and E. Sawatzky, J. Appl. Phys. **46**, 2760 (1975).
[43] R. Carey, L. Dieu, and D. M. Newman, J. Magn. Magn. Mater. **175**, 99 (1997).
[44] P. Poulopoulos, M. Angelakeris, D. Niarchos, and N. K. Flevaris, J. Magn. Magn. Mater. **140-144**, 613 (1995).
[45] R. C. Hall, J. Appl. Phys. **31**, 157S (1960).
[46] R. Zuberek, A. Wawro, H. Szymczak, A. Wisniewski, W. Paszkowicz, and M. R. J. Gibbs, J. Magn. Magn. Mater. **214**, 155 (2000).
[47] D. M. C. Nicholson, W. H. Butler, W. A. Shelton, Y. Wang, X.-G. Zhang, G. M. Stocks, and J. M. MacLaren, J. Appl. Phys. **81**, 4023 (1997).
[48] L. Néel, J. Phys. Radium **15**, 225 (1954).
[49] S. Taniguchi, Sci. Rep. Res. Inst. Tohoku Univ. A **7**, 269 (1955).
[50] A. H. MacDonald and S. Vosko, J. Phys. C **12**, 2977 (1979).
[51] A. K. Rajagopal, J. Phys. C **11**, L943 (1978).
[52] M. V. Ramana and A. K. Rajagopal, Adv. Chem. Phys. **54**, 231 (1983).
[53] P. Strange, H. Ebert, J. B. Staunton, and B. L. Gyorffy, J. Phys.: Condens. Matter **1**, 2959 (1989).
[54] B. L. Gyorffy and G. M. Stocks, Phys. Rev. Lett. **50**, 374 (1983).
[55] B. L. Gyorffy, D. D. Johnson, F. J. Pinski, D. M. Nicholson, and G. M. Stocks, in *Alloy Phase Stability*, Vol. 163 of *NATO Advanced Study Institute, Series E*: *Applied Sciences*, edited by G. M. Stocks and A. Gonis (Kluwer Academic, Dordrecht, 1987), p. 421.
[56] J. B. Staunton, D. D. Johnson, and F. J. Pinski, Phys. Rev. B **50**, 1450 (1994).
[57] J. B. Staunton, S. S. A. Razee, M. F. Ling, D. D. Johnson, and F. J. Pinski, J. Phys. D **31**, 2355 (1998).
[58] D. D. Johnson, J. B. Staunton, and F. J. Pinski, Phys. Rev. B **50**, 1473 (1994).
[59] R. Evans, Adv. Phys. **28**, 143 (1979).
[60] J.-P. Hansen and I. R. McDonald, *Theory of Simple Liquids* (Academic, New York, 1976).
[61] L. Onsager, J. Am. Chem. Soc. **58**, 1468 (1936).
[62] S. Shawcross and B. L. Gyorffy (private communication); R. V.

Chepulskii and V. N. Bugaev, Solid State Commun. **105**, 615 (1998).
[63] P. Lloyd, Proc. Phys. Soc. London **90**, 207 (1967).
[64] J. S. Faulkner and G. M. Stocks, Phys. Rev. B **21**, 3222 (1980).
[65] E. Bruno and B. Ginatempo, Phys. Rev. B **55**, 12 946 (1997).
[66] M. Hansen and K. Anderko, *Constitution of Binary Alloys* (McGraw-Hill, New York, 1958).
[67] I. V. Solovyev, P. H. Dederichs, and I. Mertig, Phys. Rev. B **52**, 13 419 (1995).
[68] J. C. A. Huang, A. C. Hsu, Y. H. Lee, T. H. Wu, and C. H. Lee, J. Appl. Phys. **85**, 5977 (1999).
[69] M. T. Lin, H. Y. Her, Y. E. Wu, C. S. Shern, J. W. Ho, C. C. Kuo, and H. L. Huang, J. Magn. Magn. Mater. **209**, 211 (2000).
[70] U. Pustogowa, J. Zabloudil, C. Uiberacker, C. Blaas, P. Weinberger, L. Szunyogh, and C. Sommers, Phys. Rev. B **60**, 414 (1999).
[71] L. Szunyogh, P. Weinberger, and C. Sommers, Phys. Rev. B **60**, 11 910 (1999).
[72] C. Leroux, M. C. Cadeville, V. Pierron-Bohnes, G. Inden, and F. Hinz, J. Phys. F: Met. Phys. **18**, 2033 (1988).
[73] A. A. Aboaf, S. R. Herd, and E. Klokholm, IEEE Trans. Magn. **MAG-19**, 1514 (1983).
[74] A. J. Freeman, R. Wu, M. Kim, and V. I. Gavrilenko, J. Magn. Magn. Mater. **203**, 1 (1999).
[75] D. Gautard, G. Couderchon, and L. Coutu, J. Magn. Magn. Mater. **160**, 359 (1996).
[76] S. Y. Chu, C. Kline, M. Q. Huang, M. E. McHenry, J. Cross, and V. G. Harris, J. Appl. Phys. **85**, 6031 (1999).
[77] J. Orehotsky, J. B. Sousa, and M. F. Pinheiro, J. Appl. Phys. **53**, 7939 (1982).
[78] F. Schedin, L. Hewitt, P. Morrall, V. N. Petrov, and G. Thornton, J. Magn. Magn. Mater. **198-199**, 555 (1999).
[79] J. B. Staunton, D. D. Johnson, and B. L. Gyorffy, J. Appl. Phys. **61**, 3693 (1987).
[80] M.-Z. Dang and D. G. Rancourt, Phys. Rev. B **53**, 2291 (1996).
[81] K. Wildberger, P. Lang, R. Zeller, and P. H. Dederichs, Phys. Rev. B **52**, 11 502 (1995).
[82] G. D. Mahan, *Many Particle Physics* (Plenum, New York, 1981).